Circulation Journal
Official Journal of the Japanese Circulation Society
http://www.j-circ.or.jp

Detrimental Impact of Vasopressin V2 Receptor Antagonism in a SU5416/Hypoxia/Normoxia-Exposed Rat Model of Pulmonary Arterial Hypertension

Itaru Goto, MD; Kaoru Dohi, MD, PhD; Yoshito Ogihara, MD; Ryuji Okamoto, MD, PhD; Norikazu Yamada, MD, PhD; Yoshihide Mitani, MD, PhD; Masaaki Ito, MD, PhD

Background: The expression of vasopressin type 2 receptor (V2R) in the lung, and the long-term effects of tolvaptan, a selective V2R antagonist, on pulmonary circulation and right ventricular (RV) remodeling in a pulmonary arterial hypertension (PAH) rat model were evaluated.

Methods and Results: Six-week-old male Sprague-Dawley rats were injected subcutaneously with 20 mg/kg of SU5416 and were exposed to hypoxia for 3 weeks followed by re-exposure to normoxia for 7 weeks. These rats showed signs of RV failure and upregulation of V2R and cAMP in the lung tissue at 10 weeks after SU5416 injection. They were then treated with either 0.05% tolvaptan in diet (SUHx+Tolv) or normal diet (SUHx) during 5–10 weeks of SU5416 injection. Normal control rats (Cont) were also used for comparison. SUHx+Tolv had significantly higher pulmonary arterial pressure, more progressive pulmonary arterial remodeling, and more severe myocyte hypertrophy and interstitial myocardial fibrosis in the right ventricle compared with SUHx despite achieving successful preload reduction.

Conclusions: Chronic vasopressin V2R antagonism may contribute to the worsening of PAH and the development of RV remodeling.

Key Words: Arginine vasopressin; Pulmonary arterial hypertension; Right ventricular failure; SU5416; Tolvaptan

Pulmonary arterial hypertension (PAH) is a progressive disease and leads to right heart failure.[1] Although endothelin-receptor antagonists, nitric oxide, phosphodiesterase type 5 inhibitors, and prostacyclin derivatives, have improved the mobility and mortality of PAH,[2–6] current therapy for right heart failure is still suboptimal. Diuretics are traditionally used to relieve congestive symptoms and to reduce edema in right heart failure secondary to PAH,[7] but it remains unknown whether administration of diuretics has long-term efficacy or extends the survival period. Arginine vasopressin (AVP) is a non-peptide hormone that is synthesized in the brain and released from the posterior pituitary gland in response to a decrease of the effective circulating blood volume. The vasopressin type 2 receptor (V2R) stimulated by AVP induces free water reabsorption via aquaporin-2 in the renal collecting duct,[8,9] and therefore selective V2R antagonist produces aquaresis that leads to clinical improvement in heart failure symptoms.[10,11] Recent experimental studies demonstrated that long-term administration of selective V2R antagonism has favorable effects on cardiac hemodynamics, and ameliorates LV remodeling and myocardial fibrosis in concert with diuretic effects in left heart failure.[12,13] In Japan, tolvaptan, a V2R antagonist, has been approved for volume overload in heart failure patients since December 2010. We recently demonstrated that 7-day treatment with 7.5 mg tolvaptan induced a significant reduction in pulmonary vascular resistance in patients with left heart failure, particularly those with high baseline values,[14,15] suggesting that V2R antagonism plays an important role in the regulation of pulmonary vascular tone. Recent clinical and research observations strongly support the existence of an extrarenal V2R, notably in the lung,[16] but as far as we know, there are few basic research reports about the long-term effects of V2R antagonism on the pulmonary circulation and right heart in PAH. We aimed to identify the physiological role of the V2R, if any, in the lung, and to investigate the long-term effects of V2 receptor antagonism on right heart failure using a PAH rat model.[17]

Methods

All experimental protocols were reviewed and approved by the Animal Care and Use Committee at the Mie University

Received November 8, 2015; revised manuscript received February 1, 2016; accepted February 3, 2016; released online February 29, 2016 Time for primary review: 7 days

Department of Cardiology and Nephrology (I.G., K.D., Y.O., R.O., N.Y., M.I.), Department of Pediatrics (Y.M.), Mie University Graduate School of Medicine, Tsu, Japan

Mailing address: Kaoru Dohi, MD, PhD, Department of Cardiology and Nephrology, Mie University Graduate School of Medicine, 2-174 Edobashi, Tsu 514-8507, Japan. E-mail: dohik@clin.medic.mie-u.ac.jp

ISSN-1346-9843 doi:10.1253/circj.CJ-15-1175

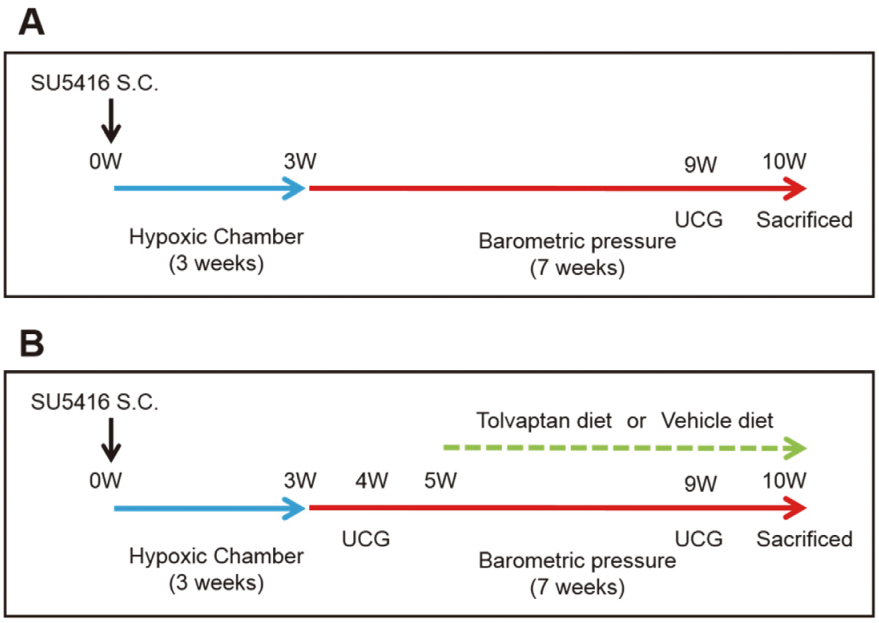

Figure 1. Diagram of the study design. (**A**) SU5416+hypoxia rats exhibited right heart failure at 9 weeks and demonstrated abundance of arginine vasopressin type2 receptor (V2R) and concentration of cAMP in lung tissue at 10 weeks. (**B**) SU5416+hypoxia rats treated with tolvaptan or vehicle for 5 weeks underwent serial echocardiography from 4 to 9 weeks after SU5416 injection. The rats were sacrificed at the end of 10 weeks after SU5416 injection.

Graduate School of Medicine and complied with the *Guide for the Care and Use of Laboratory Animals* published by the US National Institutes of Health (NIH Publication No. 85-23, revised 1985). Six-week-old male Sprague-Dawley rats (160–180 g, Japan SLC, Shizuoka, Japan) were allowed free access to tap water and standard rat chow under controlled temperature (21±1°C) and humidity (55±2%) with a 12:12-h light-dark cycle.

Experimental PAH and Right Heart Failure

The rat model of PAH was prepared for the study using established methods.[17] Rats were given a single subcutaneous injection of SU5416 (20 mg/kg) and exposed to hypoxia (10% O_2) for 3 weeks to induce PAH, and returned to normoxia (SUHx rat). A recent study demonstrated that this rat model develops very severe occlusive PAH and severe RV dysfunction, with evidence of cardiomyocyte enlargement, apoptosis, and collagen deposition during 8 weeks after a SU5416 injection.[18] To evaluate the effects of long-term V2R antagonism on pulmonary circulation and RV remodeling in much more advanced right heart failure, we decided to use SUHx rats at 9–10 weeks after a SU5416 injection.

Experimental Protocol

Rats were studied according to the protocols described below.

Protocol 1: V2R Expression and cAMP Concentration in Lung Tissue of Experimental PAH Rats Model At 10 weeks after SU5416 injection, rats (n=9) were harvested (**Figure 1A**). Their lungs were removed and prepared for semiquantitative immunoblotting of V2R and subsequent cAMP assay. Age-matched normal rats (Cont, n=8) were only injected with vehicle and kept in normoxia and normal diet during 10 weeks.

Protocol 2: Long-Term Effects of V2R Antagonism on the Development of PAH and Right Heart Failure To investigate whether V2R antagonism plays a protective role against PAH in addition to its diuretic effects for the treatment of right heart failure, the rat were treated with either 0.05% tolvaptan (Otsuka Pharmaceutical Co, Ltd, Tokyo, Japan) in the diet (SUHx+Tolv, n=16) or given a normal diet (SUHx, n=16) from 5 weeks after a SU5416 injection until the end of 10 weeks. A normal control group (Cont, n=15) was also used for comparisons. Morooka et al demonstrated that chronic treatment with 0.05% tolvaptan in the diet was associated with persistent aquaretic effects without disturbing electrolyte balances through the course in a rat hypertensive HF model, and therefore we adopted the same dosage of tolvaptan in the present study.[12] All rats in each group underwent quantitative echocardiographic evaluations at 4 and 9 weeks after SU5416 or vehicle injections. At the end of 10 weeks, rats were placed individually in metabolic cages for the assessment of fluid and food intake and urine volume for 24 h. They were then decapitated for blood collection. The remainder (n=7 in Cont, SUHx, and SUHx+Tolv, respectively) underwent hemodynamic measurements by cardiac catheterization, and their hearts and lungs were subsequently fixed for histological preparation (**Figure 1B**).

Collection of Blood, Urine, and Tissue

Rats were placed individually in metabolic cages, and urine samples were collected for 24 h at 10 weeks. Each rat was then decapitated without anesthesia, and blood from the trunk was collected into a test tube containing EDTA-2Na and centrifuged at 3,000 rpm for 15 min at 4°C to obtain blood plasma. Aliquots of urine and plasma samples were kept at –80°C. The lungs were snap frozen in liquid nitrogen and stored at –80°C. The hearts were also removed for RV and LV mass measurements.

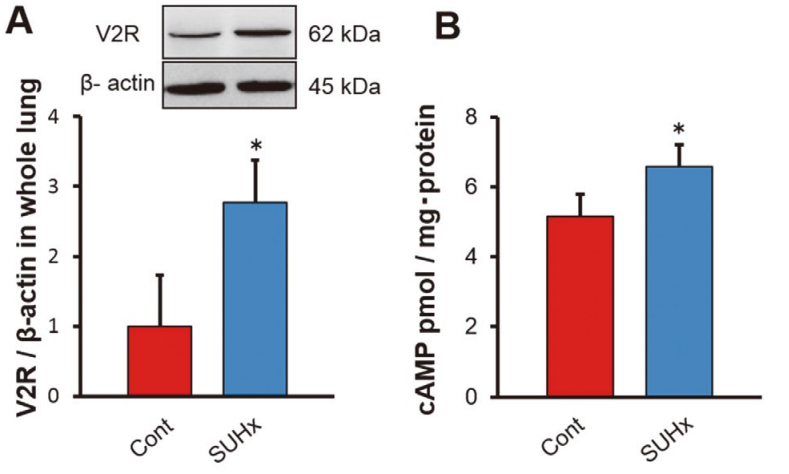

Figure 2. Semiquantitative immunoblotting and radioimmunoassay in lung tissue. (**A**) The expression of V2R in lungs (n=6 in Cont, SUHx). (**B**) The concentration of cAMP in lungs (n=8 Cont, n=9 SUHx). Cont, normal rats; SUHx, SU5416+hypoxia rats treated with a vehicle diet. Values are presented as mean±SD. *P<0.05 vs. Cont.

Quantitative Echocardiography Evaluation

Echocardiography (Vevo2100; VisualSonics, Toronto, Canada) was performed, as described previously.[19–22] Briefly, rats were anaesthetized with isoflurane (induction 3%, maintenance 0.8–1.6%) in 0.6 L/min O_2 throughout the procedure via spontaneous breathing. Heart rate (HR) was kept relatively constant throughout the procedure. Right ventricular (RV) wall thickness, RV end diastolic diameter, inferior vena cava (IVC), pulmonary arterial acceleration time/ejection time (PAAT/ET), and TAPSE were measured as described previously.[18] Doppler-derived RV cardiac output (RVCO) was also calculated.[19] Each parameter was averaged over 3 cardiac cycles.

Hemodynamic Measurements

During hemodynamic measurements, rats were anesthetized with isoflurane (induction 3%, maintenance 1.0–1.5% mixed with 100% oxygen), and the trachea was cannulated for mechanical ventilation.[23] The right carotid artery was isolated and cannulated for systemic blood pressure measurement using a micromanometer-tipped pressure transducer catheter (Millar Instruments, Houston, TX, USA). After thoracotomy, another pressure transducer catheter was inserted into the RV cavity via the RV apex and then advanced into the pulmonary artery for RV and pulmonary arterial pressure measurements, respectively. Data acquisition was performed by the Powerlab data system (AD Instruments, Colorado Springs, CO, USA).

Tissue Fixation of Lung and Heart

After hemodynamic evaluation, rats were immediately euthanized with an overdose of isoflurane. One percent formalin in phosphate-buffered saline (PBS) plus 0.5% low-melt agarose at 42°C was infused into the airway via a large-bore catheter at a constant pressure of 20 cmH_2O to keep the lung moderately distended.[24] Furthermore, 1% formalin in PBS was dripped into the right ventricle to perfuse the heart and lung until a clear effluent was obtained. The lung and heart were cooled to 4°C to allow the agarose to harden and then immersed overnight in 10% formalin in PBS. The excised heart and lung were embedded in paraffin.

Pulmonary Vascular Morphometry

Paraffin-embedded lung sections were stained with Verhoeff-Van Gieson stain for morphometric analysis.[25] The medial wall thickness (MWT) was measured at the muscular arteries (outer diameter (OD) 50–200 μm). The external diameters of small pulmonary arteries were measured along the shortest curvature. The percent MWT was calculated with the formula [(external diameter–internal diameter)/external diameter]×100] in EVG-stained slides.[26] Intra-acinar arteries (25<OD<50 μm) were categorized as muscular (those with a complete medial coat of muscle), partially muscular (those with only a crescent of muscle), or non-muscular (those with no apparent muscle).[27] All small pulmonary arteries in the left lobes of lungs from all 3 groups (n=7 in each group) were scored as one of 2 sizes (25<OD<50 μm and 50≤OD<100 μm) as follows: no evidence of neointimal formation (grade 0); partial luminal occlusion (<50%; grade 1); and severe luminal occlusion (≥50%; grade 2).[26]

Assessment of RV Cardiomyocyte Cross-Sectional Area and RV Collagen Deposition

Paraffin-embedded RV tissue sections were then stained with hematoxylin and eosin, and with Masson's trichrome for assessing myocyte size and collagen deposition, respectively. At high-power magnification (×40), 25–30 regions of photomicrographs covering the whole section were obtained and scanned for myocytes that were cut in a cross section to expose the nucleus centrally.[25,28] The cross-sectional area was measured using a KEYECE BZ-X710 microscope and BZ-X Analyzer software (Osaka, Japan). For interstitial collagen fraction quantification, blue-stained areas were determined using a color-based threshold at medium power magnification (×20).[29] The index of the interstitial fibrosis was defined as the ratio between the interstitial fibrosis area and the total surface area throughout the right ventricle.

All histological evaluations and measurements were performed by treatment-blinded investigators, and data were analyzed after all measurements were completed.

Blood and Urine Measurements

Plasma and urine electrolyte, urea nitrogen, creatinine, osmolality, and plasma renine activity and aldosterone were measured by a clinical laboratory testing service (SRL, Tokyo, Japan). ELISA kits were used for evaluating brain natriuretic peptide (BNP; AssayPro, MO, USA), angiotensin II (ANG II; Phoenix Pharmaceuticals, Inc, CA, USA), and AVP (MyBioSource, CA, USA).

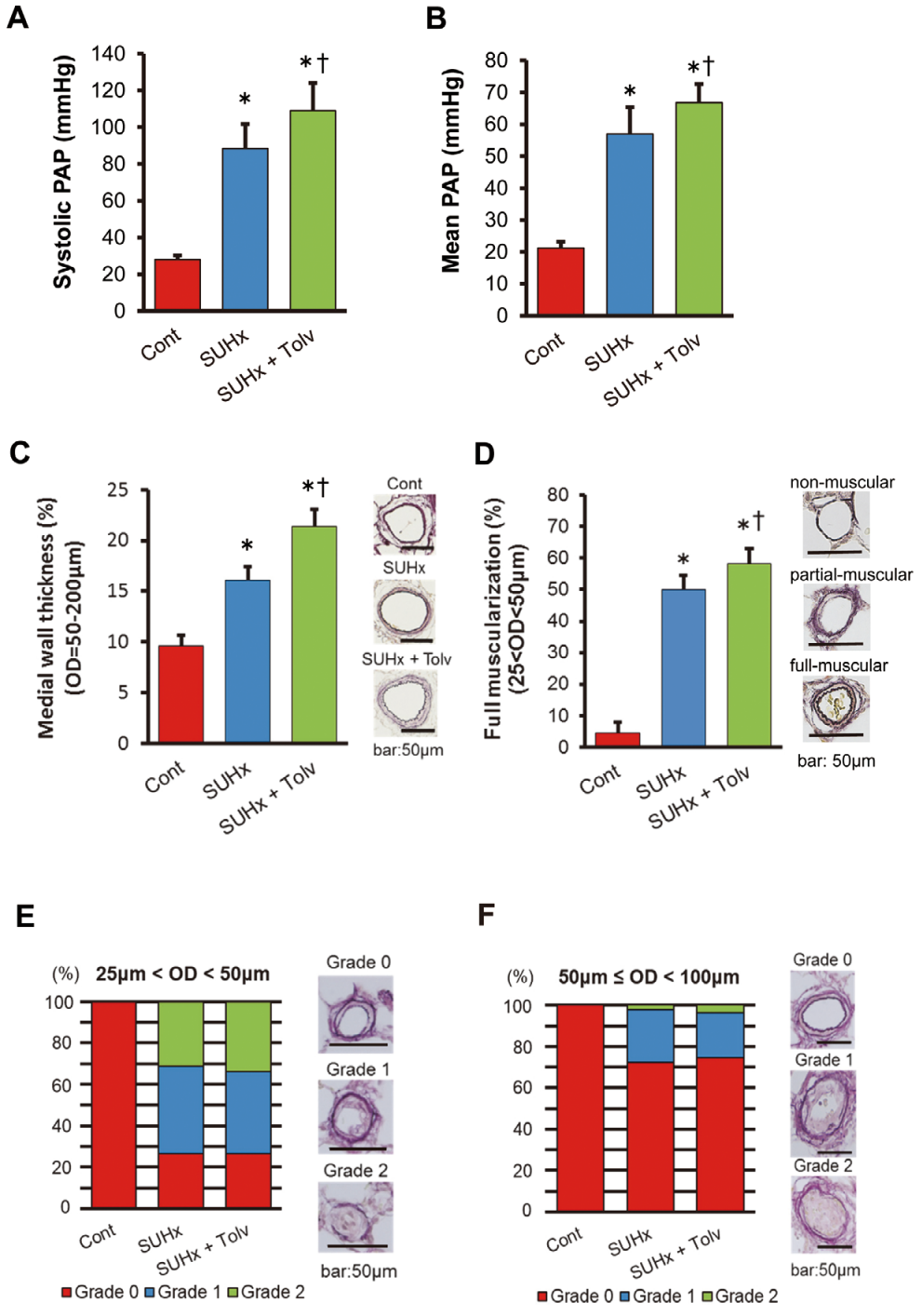

Figure 3. Hemodynamic parameters in catheterized rats and morphologic evaluation of pulmonary arteries. (**A**) Systolic pulmonary arterial pressure (systolic PAP). (**B**) Mean PAP. (**C**) The medial wall thickness (MWT) of muscular arteries (outer diameter (OD): 50–200 μm). (**D**) Percentage of fully masculalized intra-acinar arteries (25<OD<50 μm). (**E**) Percentage of grade 0 (no luminal occlusion), 1 (<50% occlusion) and 2 (≥50% occlusion) in the vessels of 25<OD<50 μm (**Left**) and representative photomicrographs of Elastic-van Gieson-stained pulmonary arterial cross-sections (**Right**). (**F**) Percentage of grade 0 (no luminal occlusion), 1 (<50% occlusion) and 2 (≥50% occlusion) in the vessels of 50≤OD<100 μm (**Left**) and representative photomicrographs of Elastic-van Gieson-stained pulmonary arterial cross-sections (**Right**). Cont, normal rats; SUHx, SU5416+hypoxia rats treated with a vehicle diet; SUHx+Tolv, SU5416+hypoxia rats treated with a tolvaptan diet. Results are presented as mean±SD. *P<0.05 vs. Cont. †P<0.05 vs. SUHx. n=7 in each groups.

Table 1. Catheter Evaluation at 10 Weeks After SU5416 Injection

	Cont (n=7)	SUHx (n=7)	SUHx+Tolv (n=7)
Heart rate (beats/min)	325.32±8.86	322.37±13.31	312.66±24.50
Systolic blood pressure (mmHg)	119.38±14.23	112.80±10.01	113.02±13.42
Systolic RV pressure (mmHg)	27.65±2.75	90.46±13.79*	110.81±15.25*,†
End-diastolic RV pressure (mmHg)	4.67±0.98	7.31±2.75	6.50±2.22

Values are presented as mean ± SD. *P<0.05 vs. Cont. †P< 0.05 vs. SUHx. Cont, normal rats; SUHx, SU5416+hypoxia rats treated with a vehicle diet; SUHx+Tolv, SU5416+hypoxia rats treated with a tolvaptan diet; RV, right ventricular.

Semiquantitative Immunoblotting

The lung tissues were individually homogenized in ice-cold RIPA buffer containing 50 mmol/L Tris–HCl, at a pH 7.4, and with 150 mmol/L NaCl, 10 mmol/L $Na_4P_2O_7$, 1 mmol/L NaF, 1 mmol/L Na_3VO_4, 1 mmol/L EDTA, 0.25% sodium deoxycholate, 1% Nonidet P-40, 1 mmol/L dithiothreitol, and 1× protease inhibitor mixture (Roche). The homogenates were centrifuged at 4,000 g for 15 min at 4°C. The supernatant was adjusted to the same final protein concentration using a BCA Protein Assay (Thermo, IL, USA) and added to 2 x SDS sample buffer. Samples were then boiled at 60°C for 10 min. These samples were separated by SDS-PAGE and transferred to a PVDF membrane, blocking with 5% skim milk in TBS-T. The Western blots were probed with antibodies to V2R (AB1797P; Millipore, Temecula, CA, USA) diluted 1:500 overnight at 4°C, and secondary antibodies (#5127; Cell signaling technology) for 1 h at room temperature, and visualized using an ECL system. The membranes were stripped and re-incubated with β-actin antibody (ab8227; Abcam). Laser densitometry (ImageQuant LAS 4000; Fuji, Tokyo, Japan) was used to quantitate the bands.

cAMP Assay

Lung tissues were homogenated in cold 0.1N HCl. The homogenates were centrifuged at 4,000 g for 15 min at 4°C. The supernatants were measured to the total protein concentration using a BCA Protein Assay. These samples were sent to a clinical laboratory testing service (SRL) for the measurement of cAMP with a Yamasa cyclic AMP RIA assay kit (YAMASA Shoyu, Chiba, Japan).

Statistical Analysis

The experimental groups were compared by using the unpaired Student's t-test or one-way analysis of variance followed by the Tukey-Kramer post-hoc test. All values were expressed as mean ± SD and values of $P < 0.05$ were considered to be statistically significant.

Results

Evidence of Right Heart Failure in the Rat PAH Model

At 9 weeks after SU5416 injection, SUHx rats developed symptoms of right heart failure including slow behavior, rapid breathing and systemic swelling, and echocardiography showed reduced cardiac output, increased RV dimension, decreased RV systolic function with leftward interventricular septal shift, and IVC dilatation due to severe PAH.

V2R Protein Level and cAMP Concentration in Lung Tissue

The V2R band was detected at 62 kDa in Western blotting. The V2R protein level in the lung was significantly higher (2.67-fold) in the SUHx compared with the Cont group (**Figure 2A**). The concentration of cAMP in the lung was significantly higher (1.27-fold) in the SUHx compared with the Cont group (**Figure 2B**).

Hemodynamic Measurement

Hemodynamic measurements at 10 weeks after a SU5416 injection revealed that both systolic and mean pulmonary arterial pressure were significantly higher in SUHx and SUHx+Tolv groups compared with those of the Cont group, and it was to a greater extent in the SUHx+Tolv group (**Figures 3A**,**B**). In contrast, there was no significant difference in systolic blood pressure or HR among the 3 groups. End-diastolic RV pressure tended to be higher in the SUHx and SUHx+Tolv groups than in the Cont group, and it was to a greater extent in the SUHx group without being statistically different (**Table 1**).

Pulmonary Vasculature

A total of 644 pulmonary arteries from 21 animals (7 rats in each group) were evaluated for MWT (OD, 50–200 μm). The percentage of MWT was significantly higher in the SUHx and SUHx+Tolv groups compared with that of the Cont group, and it was to a greater extent in the SUHx+Tolv group (**Figure 3C**). In 2,303 intra-acinar arteries in the left lung lobes, a proportion of fully muscularized vessels was significantly higher in the SUHx and SUHx+Tolv groups compared with those of the Cont group, and it was to a greater extent in the SUHx+Tolv group (**Figure 3D**). In all 7,599 small pulmonary arteries in the left lung lobes, there were no vessels with grades 1–2 in the Cont group, whereas both the SUHx and SUHx+Tolv groups had similar percentages of vessels with grades 1 and 2 in the vessels with $25<OD<50\,\mu$m and $50\leq OD<100\,\mu$m, respectively (**Figures 3E**,**F**).

Echocardiographic Measurement

Echocardiography showed RV-free wall thickening, RV chamber dilation and IVC dilation in both the SUHx and SUHx+Tolv groups at 4 weeks after SU5416 injection to a similar extent. However, the development of RV-free wall thickening, RV chamber dilation and IVC dilation was attenuated in the SUHx+Tolv group compared with the SUHx group at 9 weeks (**Figures 4A–C**), despite having similar PAAT/ET, RVCO, and TAPSE between the 2 groups (**Figures 4D–F**).

RV Remodeling

The RV/LV+Septal ratio (Fulton index) in the SUHx and SUHx+Tolv groups was significantly higher compared with those of the Cont group, and it was to a greater extent in the SUHx group (**Figure 5A**). The RV cardiomyocyte cross-sectional area and the percentage of collagen area were significantly greater in the SUHx and SUHx+Tolv groups compared with those of the Cont group, and it was to a greater extent in the SUHx+Tolv group (**Figures 5B–D**). In contrast, they were

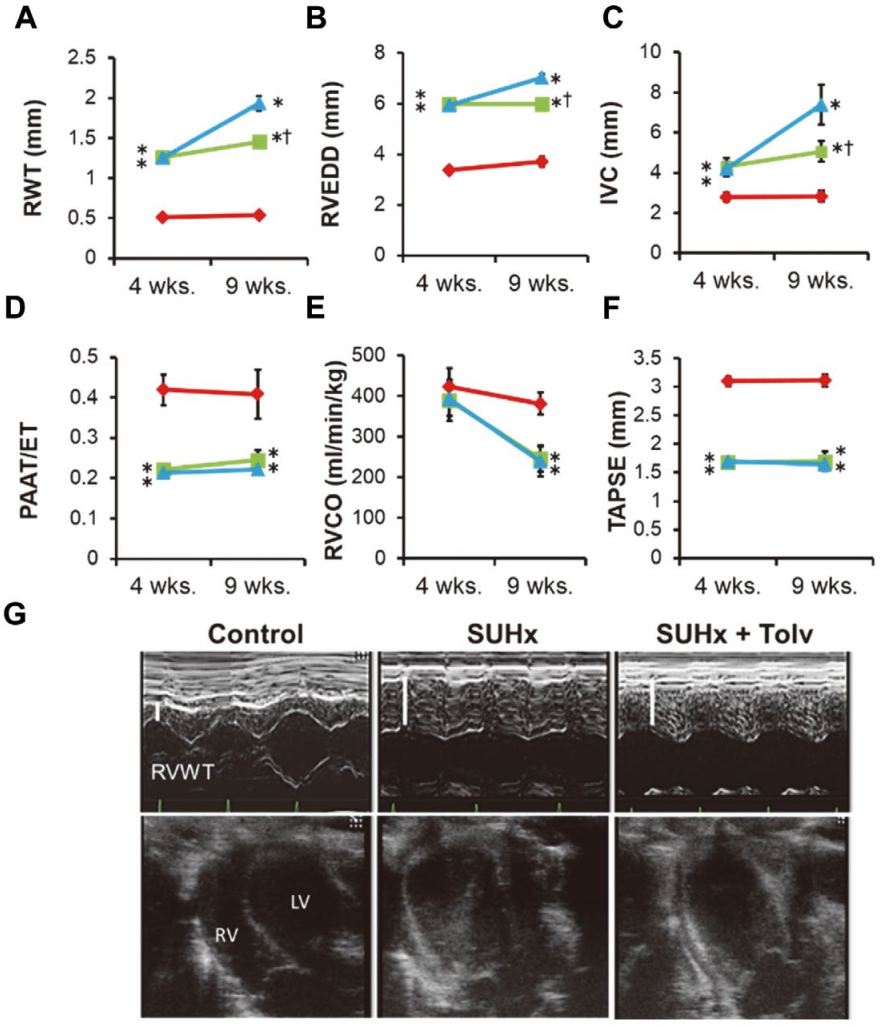

Figure 4. Evaluation of parameters in echocardiography. (**A**) Right wall thickness (RWT). (**B**) Right ventricular end-diastolic diameter (RVEDD). (**C**) Inferior vena cava (IVC). (**D**) Pulmonary arterial acceleration time/ejection time (PAAT/ET). (**E**) Right ventricular cardiac output (RVCO). (**F**) Tricuspid annular plane systolic excursion (TAPSE). Red line indicates Cont, blue line indicates SUHx, and green line indicates SUHx+Tolv. Results are presented as mean±SD. *P<0.05 vs. Cont. †P<0.05 vs. SUHx. (**G**) Representative M-mode (**Upper panel**) and B-mode (**Lower panel**) echocardiography. Cont, normal rats; SUHx, SU5416+hypoxia rats treated with a vehicle diet; SUHx+Tolv, SU5416+hypoxia rats treated with a tolvaptan diet. n=8 in each group.

similar in the LV free walls among the three groups (data not shown).

Metabolic, Blood Plasma, and Urine Parameters

Urine volume and water intake in the SUHx+Tolv group increased in the early phase after initiation of tolvaptan therapy, and remained greater in the SUHx+Tolv group than in the SUHx and Cont groups (**Table 2**). However, development of PAH caused a similar degree of weight loss in the 2 groups at 10 weeks after a SU5416 injection under the condition of free access to tap water. Blood plasma and urine biological parameters are also shown in **Table 2**. Plasma creatinine, osmolality and BNP were higher in the SUHx group compared with those in the Cont group. In the SUHx+Tolv group, these parameters were not significantly different from those of the Cont group. The plasma aldosterone level in the SUHx group was significantly higher than that in the Cont and SUHx+Tolv groups. There was no difference in plasma AVP levels among the 3 groups. Urine osmolality was not statistically different between the Cont and SUHx groups, and the SUHx+Tolv group had lower urine osmolality that the Cont group. Creatinine clearance in the SUHx and SUHx+Tolv groups was significantly lower than that in the Cont group.

Discussion

We first demonstrated that both V2R and cAMP, downstream of the V2R signal, were expressed in the lung tissue at higher levels in PAH rats than in normal rats. In contrast to the original hypothesis, chronic V2R antagonism adversely affected pulmonary vasculature, leading to increased pulmonary arterial pressure and the progression of RV remodeling. The pres-

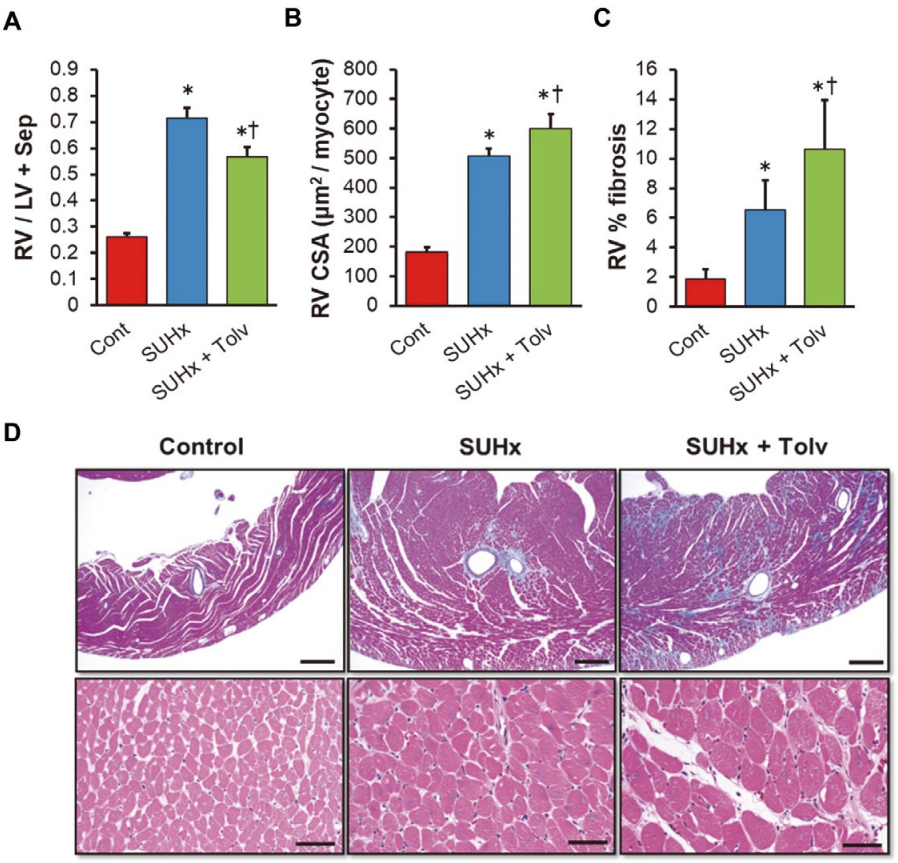

Figure 5. Morphometric evaluation of right ventricular structural remodeling. (**A**) The Fulton index (n=8 in Cont, n=9 in SUHx and SUHx+Tolv). (**B**) Right ventricular (RV) myocyte cross-section area (RV CSA) (n=7 in each group). (**C**) Quantification of collagen deposition in RV (n=7 in each group). (**D**) Representative RV sections stained with Mason trichrome for collagen assessment visualized by light microscopy (×4, bar=50 μm, **Upper panel**), and with hematoxylin & eosin for myocyte size (×40, bar=500 μm, **Lower panel**). Cont, normal rats; SUHx, SU5416+hypoxia rats treated with a vehicle diet; SUHx+Tolv, SU5416+hypoxia rats treated with a tolvaptan diet. Values are presented as mean±SD. *P<0.05 vs. Cont. †P<0.05 vs. SUHx.

ent study showed that chronic treatment with 0.05% tolvaptan in a rat PAH model induced the progression of medial wall thickening and muscularization of small pulmonary arteries, but did not accelerate intimal proliferation in pre-capillary arterioles in a rat PAH model.

Chronic V2R antagonism effectively reduced the RV preload by increasing urine volume without activation of the circulating rennin-angiotensin-aldosterone system (RAAS), resulting in a smaller RV chamber size and IVC diameter, and a lower serum BNP level compared with those without tolvaptan treatment. These apparently favorable changes, however, did not lead to regression of RV remodeling. In contrast, chronic tolvaptan treatment increased cardiomyocyte cross-sectional areas and collagen deposition areas in the right ventricle. Interestingly, the Fulton index was paradoxically lowered by tolvaptan treatment in the present study, although it in general positively correlates with pulmonary arterial pressure.[30] Toba et al recently reported that positive correlation stands until 8 weeks in the same PAH model, but the Fulton index decreased slightly while RV systolic pressure did not at 13 weeks.[26] Therefore, they speculated that this discrepancy may indicate the beginning of RV decompensation, and that excessive and long-term RV pressure overload may lead to cardiomyocyte loss.[18,23,26] In the present study, progression of PAH, preload reduction, or both, induced by V2R antagonism, can contribute to the paradoxical low Fulton index during the worsening of RV remodeling.

The direct effects of tolvaptan treatment on RV myocardium via the V2R pathway remain unclear. A previous study demonstrated that V2R may subserve endothelium-dependent vasodilation in the human forearm, but not at normal physiologic levels.[31,32] There is no laboratory evidence for the existence of V2R in the adult heart, and if any is present in the vascular endothelium, it presumably would not contribute to the pathogenesis of RV remodeling. Indeed, tolvaptan treatment did not alter cardiomyocyte cross-sectional areas and collagen deposition areas in the left ventricular free wall, suggesting no direct molecular effects of V2R pathways on the myocardial structure. In addition, the V2R-specific band was not identified by Western blotting in the heart (data not shown). Therefore, we speculated that V2R-mediated pathways do not directly cause RV remodeling. Tolvaptan has a strong diuretic effect, which ameliorates pulmonary congestion and improves pulmonary hemodynamics in left heart failure.[12,13] In contrast,

Table 2. Metabolic, Biochemical, Hormonal, and Urine Parameters in SUHx Rats Treated With Vehicle or Tolvaptan at 10 Weeks After SU5416 Injection

	Cont (n=8)	SUHx (n=9)	SUHx+Tolv (n=9)
Metabolic parameters			
Body weight (g)	470.6±39.2	357.5±50.6*	381.2±40.5*
Fluid intake (ml/day)	22.8±6.2	23.4±5.1	31.9±8.9*,†
Urinary volume (ml/day)	11.4±4.5	13.4±4.4	18.6±4.2*,†
Food consumption (g/day)	10.8±4.7	11.8±2.8	14.0±4.7
Plasma parameters			
Sodium (mEq/L)	148.9±1.9	149.1±5.5	150.3±3.8
Chloride (mEq/L)	93.9±2.4	93.2±3.4	95.1±2.3
Urea nitrogen (mg/dl)	17.2±2.9	29.1±5.0*	26.4±5.0*
Creatinine (mg/dl)	0.27±0.03	0.44±0.14*	0.36±0.06
Osmolality (mOsm/H_2O)	295.3±4.1	306.2±10.0*	303.0±6.7
Brain natriuretic peptide (pg/ml)	100.8±13.7	165.8±83.1*	113.6±24.7
Plasma renin activity ($ng \cdot ml^{-1} \cdot h^{-1}$)	3.18±0.87	4.86±3.58	3.79±2.14
Angiotensin II (pg/ml)	686.0±331.6	893.8±630.9	780.6±462.3
Aldosterone (pg/ml)	250.0±112.7	506.7±238.4*	200.1±149.9†
Arginine vasopressin (pg/ml)	6.28±0.31	6.40±0.34	6.35±0.53
Urine parameters			
Osmolality (mOsm/H_2O)	1,471.3±514.2	1,253.3±252.4	1,018.7±147.3*
Sodium (mEq/day)	0.79±0.33	0.76±0.33	0.88±0.43
Potassium (mEq/day)	2.00±0.82	2.13±0.61	2.46±0.61
Chloride (mEq/day)	0.84±0.47	0.90±0.41	0.95±0.43
Nitrogen (mg/day)	267.6±81.3	272.5±73.0	314.9±47.4
Creatinine (mg/day)	16.2±1.6	11.8±3.3*	13.2±2.4
Creatinine clearance (ml/min)	4.30±0.66	2.01±0.81*	2.63±0.87*
FENa (%)	0.09±0.03	0.18±0.09*	0.16±0.09

Values are presented as mean±SD. *P<0.05 vs. Cont. †P<0.05 vs. SUHx. FENa, fractional excretion of sodium. Other abbreviations as in Table 1.

progression of pulmonary artery remodeling induced by V2R antagonism could surpass its favorable volume depletion effect in the treatment of PAH and right heart failure.

Study Limitations

The underlying mechanisms responsible for muscularization and medial thickening of small pulmonary arteries and via V2R antagonism remain unclear. V2R was identified in the cultured pulmonary arterial smooth muscle cells (PASMCs) from humans and Sprague-Dawley rats by immunofluorescence staining (**Figure S1A**: performed only in rat PASMCs) and Western blotting (**Figure S1B**), but proliferation of PASMCs and cyclic AMP concentration in rat PASMCs was unchanged by V2R stimulation with or without tolvaptan administration (**Figures S1C,D**). Although cultured PAH-PASMCs from intra-acinar arteries were not examined, these results indicate that the V2R-cAMP pathways may have no direct effect on the proliferation of PASMCs. As both V2R protein level and concentration of cAMP in the whole lung tissue was significantly higher in the SUHx group compared with the Cont group, stimulation of the V2R-cAMP pathways in non-PASMCs may lead to PASMC proliferation and/or endothelial-to-mesenchymal transition via undetected molecular or hemodynamic mechanisms,[33] whereas tolvaptan treatment did not influence cell signaling pathways mediated by pulmonary arterial endothelial cells and secretion of cytokines/chemokines/growth factors (**Figures S2A–E**). Although tolvaptan did not activate the circulating RAAS activity, the effects of V2R antagonism on the local RAAS activity in the lung and heart were not investigated in the present study.[34] Unlike left heart failure,[35] the pathophysiological role of local RAAS on RV function and remodeling during the progression of PAH remains under investigation.[36] We did not elucidate the role of V2R in the pathogenesis of PAH using other models of PAH including monocrotaline-induced and hypoxia-induced PAH in rats or other species including humans. We did not evaluate the effects of tolvaptan on pulmonary vasculature in non-PAH rats. Finally, our study did not focus on the short-term effects of V2R antagonism for the treatment of excessive fluid overload and systemic congestion at various time points during the progression of PAH.

In conclusion, the present study offers in vivo evidence of the adverse effects of long-term V2R antagonism on pulmonary circulation and RV remodeling in PAH despite achieving successful preload reduction.

Acknowledgments

The tolvaptan diet was generously provided by Otsuka Pharmaceutical Co, Ltd (Tokyo, Japan). We are grateful to Eri Nakashima, and Rie Ito for their excellent technical assistance.

Disclosures

K.D. received lecture fees of equal to or more than 500,000 yen from Otsuka Pharma Inc. in 2014. N.Y. received lecture fees of more than 500,000 yen from Daiichi Sankyo Co Ltd and Astellas Pharma Inc in 2014. M.I. received lecture fees of more than 500,000 yen from Daiichi Sankyo Co Ltd in 2014. M.I. received a single-year unrestricted research grant from the Department of Cardiology and Nephrology, Mie University Graduate School of Medicine, of equal to or more than 2 million yen,

from Astellas Pharma Inc, Pfizer Inc, Takeda Pharmaceutical Co Ltd, Daiichi Sankyo Co Ltd, Sumitomo Dainippon Pharma Co Ltd and the Public Health Research Foundation in 2014.

No relevant conflicts of interest were disclosed by the authors.

References

1. Benza RL, Miller DP, Barst RJ, Badesch DB, Frost AE, McGoon MD. An evaluation of long-term survival from time of diagnosis in pulmonary arterial hypertension from the REVEAL Registry. *Chest* 2012; **142:** 448–456.
2. Humbert M, Sitbon O, Simonneau G. Treatment of pulmonary arterial hypertension. *N Engl J Med* 2004; **351:** 1425–1436.
3. Channick RN, Simonneau G, Sitbon O, Robbins IM, Frost A, Tapson VF, et al. Effects of the dual endothelin-receptor antagonist bosentan in patients with pulmonary hypertension: A randomised placebo-controlled study. *Lancet* 2001; **358:** 1119–1123.
4. Galiè N, Ghofrani HA, Torbicki A, Barst RJ, Rubin LJ, Badesch D, et al. Sildenafil citrate therapy for pulmonary arterial hypertension. *N Engl J Med* 2005; **353:** 2148–2157.
5. Barst RJ, Rubin LJ, McGoon MD, Caldwell EJ, Long WA, Levy PS. Survival in primary pulmonary hypertension with long-term continuous intravenous prostacyclin. *Ann Intern Med* 1994; **121:** 409–415.
6. Elias-Al-Mamun M, Satoh K, Tanaka S, Shimizu T, Nergui S, Miyata S, et al. Combination therapy with fasudil and sildenafil ameliorates monocrotaline-induced pulmonary hypertension and survival in rats. *Circ J* 2014; **78:** 967–976.
7. Galiè N, Corris PA, Frost A, Girgis RE, Granton J, Jing ZC, et al. Updated treatment algorithm of pulmonary arterial hypertension. *J Am Coll Cardiol* 2013; **62:** D60–D72.
8. Nonoguchi H, Owada A, Kobayashi N, Takayama M, Terada Y, Koike J, et al. Immunohistochemical localization of V2 vasopressin receptor along the nephron and functional role of luminal V2 receptor in terminal inner medullary collecting ducts. *J Clin Invest* 1995; **96:** 1768–1778.
9. Nielsen S, Chou CL, Marples D, Christensen EI, Kishore BK, Knepper MA. Vasopressin increases water permeability of kidney collecting duct by inducing translocation of aquaporin-CD water channels to plasma membrane. *Proc Natl Acad Sci USA* 1995; **92:** 1013–1017.
10. Kinugawa K, Sato N, Inomata T, Shimakawa T, Iwatake N, Mizuguchi K. Efficacy and safety of tolvaptan in heart failure patients with volume overload. *Circ J* 2014; **78:** 844–852.
11. Dohi K, Watanabe K, Ito M. Urine osmolality-guided tolvaptan therapy in decompensated heart failure. *Circ J* 2013; **77:** 313–314.
12. Morooka H, Iwanaga Y, Tamaki Y, Takase T, Akahoshi Y, Nakano Y, et al. Chronic administration of oral vasopressin type 2 receptor antagonist tolvaptan exerts both myocardial and renal protective effects in rats with hypertensive heart failure. *Circ Heart Fail* 2012; **5:** 484–492.
13. Yamazaki T, Izumi Y, Nakamura Y, Yamashita N, Fujiki H, Osada-Oka M, et al. Tolvaptan improves left ventricular dysfunction after myocardial infarction in rats. *Circ Heart Fail* 2012; **5:** 794–802.
14. Dohi K, Ito M. Immediate and short-term use of tolvaptan for acute decompensated heart failure. *Circ J* 2014; **78:** 829–831.
15. Watanabe K, Dohi K, Sugimoto T, Yamada T, Sato Y, Ichikawa K, et al. Short-term effects of low-dose tolvaptan on hemodynamic parameters in patients with chronic heart failure. *J Cardiol* 2012; **60:** 462–469.
16. Juul KV, Bichet DG, Nielsen S, Nørgaard JP. The physiological and pathophysiological functions of renal and extrarenal vasopressin V2 receptors. *Am J Physiol Renal Physiol* 2014; **306:** F931–F940.
17. Abe K, Toba M, Alzoubi A, Ito M, Fagan KA, Cool CD, et al. Formation of plexiform lesions in experimental severe pulmonary arterial hypertension. *Circulation* 2010; **121:** 2747–2754.
18. Alzoubi A, Toba M, Abe K, O'Neill KD, Rocic P, Fagan KA, et al. Dehydroepiandrosterone restores right ventricular structure and function in rats with severe pulmonary arterial hypertension. *Am J Physiol Heart Circ Physiol* 2013; **304:** H1708–H1718.
19. Liu J, Rigel DF. Echocardiographic examination in rats and mice. *Methods Mol Biol* 2009; **573:** 139–155.
20. Hardziyenka M, Campian ME, de Bruin-Bon HA, Michel MC, Tan HL. Sequence of echocardiographic changes during development of right ventricular failure in rat. *J Am Soc Echocardiogr* 2006; **19:** 1272–1279.
21. Ichikawa K, Dohi K, Sugiura E, Sugimoto T, Takamura T, Ogihara Y, et al. Ventricular function and dyssynchrony quantified by speckle-tracking echocardiography in patients with acute and chronic right ventricular pressure overload. *J Am Soc Echocardiogr* 2013; **26:** 483–492.
22. Vieillard-Baron A, Loubieres Y, Schmitt JM, Page B, Dubourg O, Jardin F. Cyclic changes in right ventricular output impedance during mechanical ventilation. *J Appl Physiol* 1999; **87:** 1644–1650.
23. Pacher P, Nagayama T, Mukhopadhyay P, Bátkai S, Kass DA. Measurement of cardiac function using pressure-volume conductance catheter technique in mice and rats. *Nat Protoc* 2008; **3:** 1422–1434.
24. Halbower AC, Mason RJ, Abman SH, Tuder RM. Agarose infiltration improves morphology of cryostat sections of lung. *Lab Invest* 1994; **71:** 149–153.
25. Preston IR, Sagliani KD, Warburton RR, Hill NS, Fanburg BL, Jaffe IZ. Mineralocorticoid receptor antagonism attenuates experimental pulmonary hypertension. *Am J Physiol Lung Cell Mol Physiol* 2013; **304:** L678–L688.
26. Toba M, Alzoubi A, O'Neill KD, Gairhe S, Matsumoto Y, Oshima K, et al. Temporal hemodynamic and histological progression in Sugen5416/hypoxia/normoxia-exposed pulmonary arterial hypertensive rats. *Am J Physiol Heart Circ Physiol* 2014; **306:** H243–H250.
27. Akagi S, Nakamura K, Matsubara H, Kondo M, Miura D, Matoba T, et al. Intratracheal administration of prostacyclin analog-incorporated nanoparticles ameliorates the development of monocrotaline and sugen/hypoxia-induced pulmonary arterial hypertension. *J Cardiovasc Pharmacol* 2016 January 7, doi:10.1097/FJC.0000000000000352.
28. Chintalgattu V, Ai D, Langley RR, Zhang J, Bankson JA, Shih TL, et al. Cardiomyocyte PDGFR-beta signaling is an essential component of the mouse cardiac response to load-induced stress. *J Clin Invest* 2010; **120:** 472–484.
29. Teekakirikul P, Eminaga S, Toka O, Alcalai R, Wang L, Wakimoto H, et al. Cardiac fibrosis in mice with hypertrophic cardiomyopathy is mediated by non-myocyte proliferation and requires Tgf-β. *J Clin Invest* 2010; **120:** 3520–3529.
30. Sawada H, Mitani Y, Maruyama J, Jiang BH, Ikeyama Y, Dida FA, et al. A nuclear factor-kappaB inhibitor pyrrolidine dithiocarbamate ameliorates pulmonary hypertension in rats. *Chest* 2007; **132:** 1265–1274.
31. Hirsch AT, Dzau VJ, Majzoub JA, Creager MA. Vasopressin-mediated forearm vasodilation in normal humans: Evidence for a vascular vasopressin V2 receptor. *J Clin Invest* 1989; **84:** 418–426.
32. Goldsmith SR, Gheorghiade M. Vasopressin antagonism in heart failure. *J Am Coll Cardiol* 2005; **46:** 1785–1791.
33. Xiong J. To be EndMT or not to be, that is the question in pulmonary hypertension. *Protein Cell* 2015; **6:** 547–550.
34. de Man FS, Tu L, Handoko ML, Rain S, Ruiter G, François C, et al. Dysregulated renin-angiotensin-aldosterone system contributes to pulmonary arterial hypertension. *Am J Respir Crit Care Med* 2012; **186:** 780–789.
35. Komajda M. Current challenges in the management of heart failure. *Circ J* 2015; **79:** 948–953.
36. Gomez-Arroyo J, Sandoval J, Simon MA, Dominguez-Cano E, Voelkel NF, Bogaard HJ. Treatment for pulmonary arterial hypertension-associated right ventricular dysfunction. *Ann Am Thorac Soc* 2014; **11:** 1101–1115.

Supplementary Files

Supplementary File 1

Methods

Figure S1. (**A**) Rat pulmonary artery smooth muscle cells (PASMCs) immunofluorescence staining for vasopressin V2 receptor (V2R).

Figure S2. Western blotting analysis of (**A**) endothelial NOS phosphorylation ratio, (**B**) endothelin-1/β-actin ratio, (**C**) vascular endothelial growth factor/β-actin ratio, (**D**) collagen tissue growth factor/β-actin ratio and (**E**) mature transforming growth factor-β1/β-actin ratio.

Please find supplementary file(s);
http://dx.doi.org/10.1253/circj.CJ-15-1175